

# Study on Exploration of Azeotropic Point of Pb-Sb Alloys by Vacuum Distillation and *Ab Initio* Molecular Dynamic Simulation



BINGYI SONG, WENLONG JIANG, BIN YANG, XIUMIN CHEN, BAOQIANG XU, LINGXIN KONG, DACHUN LIU, and YONGNIAN DAI

The possibility of the separation of Pb-Sb alloys by vacuum distillation was investigated theoretically. The results show that Pb and Sb can be separated by vacuum distillation. However, the experimental results show that vacuum distillation technique does not provide clear separation. According to the literature, Pb-Sb alloys belong to azeotropic compounds under some certain temperature; the experiment and computer simulation were carried out based on the exceptional condition so as to analyze the reason from the experiment and microstructure of Pb-Sb alloys perspective. The separation of Pb-Sb alloys by vacuum distillation was experimentally carried out to probe the azeotropic point. Also, the functions, such as partial radial distributions functions, the structure factor, mean square displacement, and the density of state, were calculated by *ab-initio* molecular dynamics for the representation of the structure and properties of Pb-Sb alloys with different composition of Sb. The experimental results indicate that there exists common volatilization for Pb-Sb alloys when Sb content is 16.5 wt pct. On the other hand, the calculation results show that there is an intense interaction between Pb and Sb when Sb content is 22 wt pct, which supports the experimental results although Sb content is slightly deviation.

DOI: 10.1007/s11661-016-3663-8

© The Minerals, Metals & Materials Society and ASM International 2016

## I. INTRODUCTION

ENORMOUS Pb-based alloys such as Pb-Sb and Pb-Sn have been accumulated from tin smelters and the recycle of secondary metals. Furthermore, high-effective utilization of secondary resource and the increasing demand for Sb have got considerable interest in the separation of Pb-based alloys. However, there are some serious problems in conventional methods such as low recovery of metals, high energy consumption, and evident environment pollution.<sup>[1,2]</sup>

Dai *et al.*<sup>[3-7]</sup> have studied the separation of high-lead-antimony alloys (Sb ~ 90 pct, Pb ~ 10 pct) by vacuum distillation, showed that the method is feasible, and the effect is better. However, an abnormal phenomenon in the process separation of Pb-Sb alloys has been reported. Zhang<sup>[8]</sup> found that there was no

difference of the Sb content between in vapor phase and liquid phase, while Sb content was 22 wt pct at 1073 K (800 °C); meanwhile, similar conclusions were presented by Yang<sup>[7]</sup> and Hu,<sup>[9]</sup> and they pointed out that Sb and Pb simultaneously evaporated into vapor phase when Sb content was 20 to 25, and 23 wt pct at 1073 K (800 °C), respectively. Furthermore, Kroll<sup>[10]</sup> also proposed that there existed an azeotropy at a certain composition (about 75 pct Pb), *viz.* the metal and the metal vapor had the same composition. The experimental results quoted above indicate that the presence of azeotropes causes the appearance of separating manifolds of various ingredients, which prevents the obtainment of fractions of the required composition. Above studies focused on their experiments, unfortunately, there are not many researches on their theoretical researches, especially the molecular dimension of the simulation.

Kumar<sup>[11]</sup> have reported the structure and stability of liquid Pb-Sb alloys determined by the Kumar-Samarin technique of centrifuging liquid metals. It was observed that liquid Pb-Sb alloys in the composition ranges 0 to 5 and 65 to 100 at pct Sb were stable and can be regarded as a colloidal dispersion of lead- and antimony-rich clusters in monatomic matrices. Guo<sup>[12]</sup> have measured electrical resistivity and viscosity of Pb-Sb alloys to investigate Peierls distortion behavior in the melts, which indicated that abnormal structure transition was attributed to the formation of large Sb clusters with Peierls distortion in Pb<sub>30</sub>Sb<sub>70</sub> and Pb<sub>20</sub>Sb<sub>80</sub> melts. Bian<sup>[13]</sup> have investigated an abnormal zone above the equilibrium liquidus of Pb-Sb alloy by thermal

---

BINGYI SONG and LINGXIN KONG, Ph.D. Candidates, WENLONG JIANG, Lecturer, BIN YANG, XIUMIN CHEN, BAOQIANG XU, and DACHUN LIU, Professors, are with the National Engineering Laboratory for Vacuum Metallurgy, Kunming University of Science and Technology, No 253#, Xuefu Road, Kunming, 650093, P.R. China, and with the Key Laboratory for Nonferrous Vacuum Metallurgy of Yunnan Province, Kunming 650093, P.R. China, and also with the State Key Laboratory of Complex Nonferrous Metal Resources Clear Utilization, Kunming University of Science and Technology. Contact e-mail: jiangwlkg@foxmail.com YONGNIAN DAI, Academician, is with the National Engineering Laboratory for Vacuum Metallurgy, Kunming University of Science and Technology.

Manuscript submitted July 8, 2014.

Article published online July 25, 2016

**Table I. The Activity Coefficients of Pb-Sb Alloys at Different Temperatures**

$x_{Pb}$	Experiment			MIVM											
	905 K (632 °C) <sup>[35]</sup>			905 K (632 °C)		873 K (600 °C)		973 K (700 °C)		1073 K (800 °C)		1173 K (900 °C)		1273 K (1000 °C)	
	$\gamma_{Pb}$	$\gamma_{Sb}$		$\gamma_{Pb}$	$\gamma_{Sb}$	$\gamma_{Pb}$	$\gamma_{Sb}$	$\gamma_{Pb}$	$\gamma_{Sb}$	$\gamma_{Pb}$	$\gamma_{Sb}$	$\gamma_{Pb}$	$\gamma_{Sb}$	$\gamma_{Pb}$	$\gamma_{Sb}$
0.1	0.817	0.998		0.8170	0.9976	0.8170	0.9976	0.8160	0.9974	0.8150	0.9974	0.8150	0.9974	0.8140	0.9974
0.2	0.852	0.990		0.8525	0.9900	0.8525	0.9901	0.8520	0.9900	0.8515	0.9899	0.8510	0.9898	0.8505	0.9898
0.3	0.885	0.978		0.8850	0.9777	0.8850	0.9779	0.8847	0.9776	0.8843	0.9774	0.8840	0.9773	0.8840	0.9771
0.4	0.914	0.961		0.9140	0.9608	0.9140	0.9610	0.9140	0.9607	0.9138	0.9603	0.9138	0.9600	0.9138	0.9598
0.5	0.939	0.939		0.9394	0.9394	0.9394	0.9396	0.9394	0.9392	0.9394	0.9388	0.9394	0.9384	0.9394	0.9382
0.6	0.961	0.914		0.9608	0.9140	0.9608	0.9143	0.9608	0.9138	0.9610	0.9133	0.9610	0.9130	0.9610	0.9125
0.7	0.978	0.885		0.9777	0.8850	0.9777	0.8850	0.9779	0.8847	0.9779	0.8840	0.9779	0.8837	0.9780	0.8833
0.8	0.99	0.852		0.9900	0.8525	0.9900	0.8525	0.9901	0.8520	0.9901	0.8515	0.9901	0.8515	0.9901	0.8510
0.9	0.998	0.817		0.9976	0.8170	0.9974	0.8170	0.9976	0.8170	0.9976	0.8170	0.9976	0.8160	0.9976	0.8160

differential analysis and electrical resistivity experiment. It turned out that the sudden change in electrical resistivity was owing to the electrical resistivity of liquid metals relating to structure factors. Studies focusing on simulating Pb-Sb alloys by *ab initio* molecular dynamics remain scarce in the literature. Molecular dynamics simulation provides the methodology for detailed microscopic modeling on the molecular scale, and the existence of some azeotropes may be obvious from simulation results in certain instances.<sup>[14]</sup>

Against this background, it was decided to investigate the structure and stability of liquid lead-antimony alloys by *ab initio* molecular dynamics simulation. An *ab initio* molecular dynamics simulation (AIMD) is a very effective and successful tool for describing liquid alloys, in which the correlation between the ionic configuration and the electronic states plays an important role.<sup>[15]</sup> Recently, AIMD has been applied to several liquid alloys<sup>[16-22]</sup> and made a contribution to a better understanding of these liquid alloys.

In this paper, we reproduced the experiment at 1073 K (800 °C), and we applied an *ab initio* molecular dynamic simulation to liquid Pb-Sb alloys. The purpose of this study was to provide a microscopic interpretation for the observed characteristic features in order to explain the abnormal phenomenon of Pb-Sb alloy.

## II. THEORETICAL BASIS

### A. Vapor-Liquid Equilibrium Diagram

In order to quantitatively estimate the distribution of elements in vapor and liquid phase at a certain temperature and composition, Dai Yongnian<sup>[2]</sup> proposed vapor-liquid phase equilibrium diagram. Its expression is as follows:

$$Pb_g = \left[ 1 + \left( \frac{Sb_l}{Pb_l} \right) \cdot \left( \frac{\gamma_{Sb}}{\gamma_{Pb}} \right) \cdot \left( \frac{P_{Sb}^*}{P_{Pb}^*} \right) \right]^{-1} \quad [1]$$

The activity coefficient required for Eq. [1] can be calculated by molecular interaction volume model (MIVM),<sup>[23]</sup> where  $Pb_g$ ,  $Pb_l$  and  $Sb_l$  are the mass

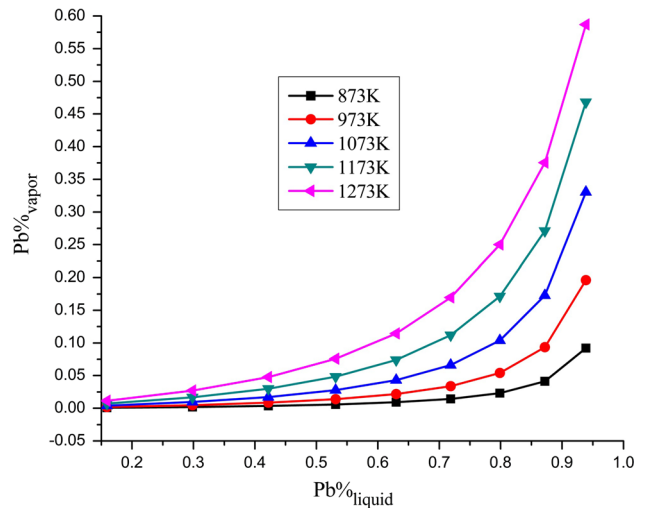


Fig. 1—The vapor-liquid phase diagram of Pb-Sb alloys at different temperatures.

fraction of Pb and Sb, the subscripts g and l represent vapor and liquid phase;  $\gamma_{Pb}$  and  $\gamma_{Sb}$  are the activity coefficient of Pb and Sb components;  $p_{Pb}^*$  and  $p_{Sb}^*$  are the saturated vapor pressures of Pb and Sb in pure state, respectively. And  $Sb_l/Pb_l$  is the mass ratio of component Sb in liquid phase to that of Pb.

The results are listed in Table I.

It can be seen from table that the predicted values are in good agreement with the experimental data. This shows that the temperature has little effect on the activity coefficient, namely, MIVM can be well applied in Pb-Sb system. Thus, vapor-liquid phase equilibrium diagram can be calculated according the Eq. [1], plotted in Figure 1.

In Figure 1, the Pb content in vapor phase increases with the increasing temperature for the fixed Pb content in liquid phase. And at the same temperature, Pb content in vapor phase show rapid growth trend. The content of Pb in vapor phase was 0.33 wt pct, while in liquid phase, it was 94 wt pct at 1073 K (800 °C). This behavior indicates that Pb will evaporate into vapor phase, while Sb remains in the liquid and, so Pb and Sb cannot be separated completely.

### III. METHODS

#### A. Experiment Methods

##### 1. Materials and equipments

Pure Pb (99.29 wt pct) and pure Sb (99.95 wt pct) were used for fusion alloying with the component of Pb-11.2 wt pctSb, Pb-16.5 wt pctSb, Pb-20 wt pctSb, Pb-22 wt pctSb, and Pb-50 wt pctSb, respectively. The vertical vacuum furnace was used for vacuum distillation, and the schematic sketch of the furnace is shown in Figure 2.

##### 2. Experimental procedure

The separation of Pb-Sb alloys was carried out in a clean room of vacuum furnace. In the process of distillation, nearly 150 g of raw Pb-Sb alloy was loaded into the bottom graphite crucible and placed inside the vacuum furnace, which was then evacuated to a vacuum of 10 to 30 Pa using vacuum pump. The temperature was increased to the target temperature and then thermal insulation for a period of time. After completion of the distillation process, the furnace was cooled to room temperature to solidify, respectively, the purified residue Pb and the volatile Sb. Water cooling system was working over the process.

Finally, the samples were collected from the volatile and residue. Flame atomic absorption spectroscopy (FAAS) and chemical analysis methods were used to analyze the contents of Pb and Sb in both residue and volatile.

#### B. Computational Methods

The present calculations have been performed with Cambridge Serial Total Energy Package code of Materials Studio, which is based on density functional theory within the generalized gradient approximation using the PBE functional due to Perdew, Burke, and Ernzerhof.<sup>[24]</sup> And the ultrasoft pseudopotentials have been used to describe the electron-ion interaction. The supercell approach with periodic boundary conditions is used to study properties. All the simulations have been

performed in a canonical ensemble with a Nosé-Hoover thermostat for temperature control and Andersen for pressure control. In addition,  $6s^2$  plus  $6p^2$  states for Pb and  $5s^2$  plus  $5p^3$  states for Sb have been regarded as valence electrons. In this work, our simulations for liquid Pb-Sb with different component have been performed in a supercell containing 108 Pb and Sb atoms. They have been randomly arranged in the simple-cubic supercell as the initial configuration. Then, an AIMD simulation run has been performed 1000 steps (1 ps of simulated time) and carried out using NPT ensemble at the temperature of 1073 K (800 °C).

### IV. RESULTS AND DISCUSSIONS

#### A. Experiment Results

The quantitative analysis has been carried out by FAAS and chemical analysis method, which are given in Table II.

In Table II, five groups of experiments are taken into consider. For Pb-11.2 wt pctSb alloy, the Sb content is larger in liquid phase than in vapor phase, and the ratio of Pb/Sb is less in residue than in volatile. For Pb-16.5 wt pctSb alloy, the Sb content in vapor and liquid phase are in equilibrium, and the ratio of Pb/Sb in residue and volatile is equal. In addition, the Sb content is less in liquid phase than in vapor phase for Pb-20 wt pctSb, Pb-22 wt pctSb, and Pb-50 wt pctSb, and the ratio of Pb/Sb is larger in residue than in volatile, respectively. Therefore, we believe that Pb-16.5 wt pctSb is azeotropic point.

#### B. Simulation Results

##### 1. Electronic properties

The structural behaviors of liquid alloys can be understood in terms of the electronic structure. AIMD simulations for the liquid alloys of Pb-15 wt pctSb, Pb-17.7 wt pctSb, Pb-18.4 wt pctSb, Pb-19.8 wt pctSb, Pb-22 wt pctSb, Pb-25.7 wt pctSb, and Pb-29.6 wt pctSb have been carried out. The partial electronic density of states (PDOS) is calculated by sampling 1 k-point of the Brillouin zone. Figure 3 shows PDOS of the alloys at 1073 K (800 °C). A sharp peak from  $-18$  to  $-16$  eV was ignored in order to illustrate the peaks nearby Fermi level better.

In Figure 3, PDOS curve generated clearly shows a metallic behavior, and a gap of about 2.0 eV separating a lower *s*-like and an upper *p*-like band, in keeping with the CMD predictions by Jank and Hafner,<sup>[25]</sup> the AIMD results by Knider,<sup>[26]</sup> and AIMD predictions by Alemany<sup>[27]</sup> using real-space pseudopotentials, AIMD simulations by Hao.<sup>[28]</sup> The existence of such a gap is in agreement with conclusions drawn on the basis of photoemission spectra results.<sup>[27]</sup>

PDOS curve consists of two wide bands, the energy region  $-12.5 < E < -6$  eV is determined primarily by the *s*-orbital, while the  $-4$  eV  $< E < 3.8$  eV is dominated by the *p*-state of these alloys. For 22 wt pctSb, its band width nearby Fermi level narrows, corresponding

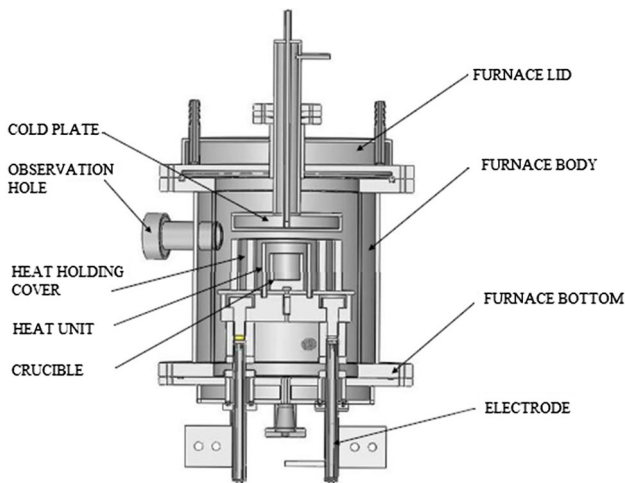


Fig. 2—Schematic diagram of vertical vacuum furnace.

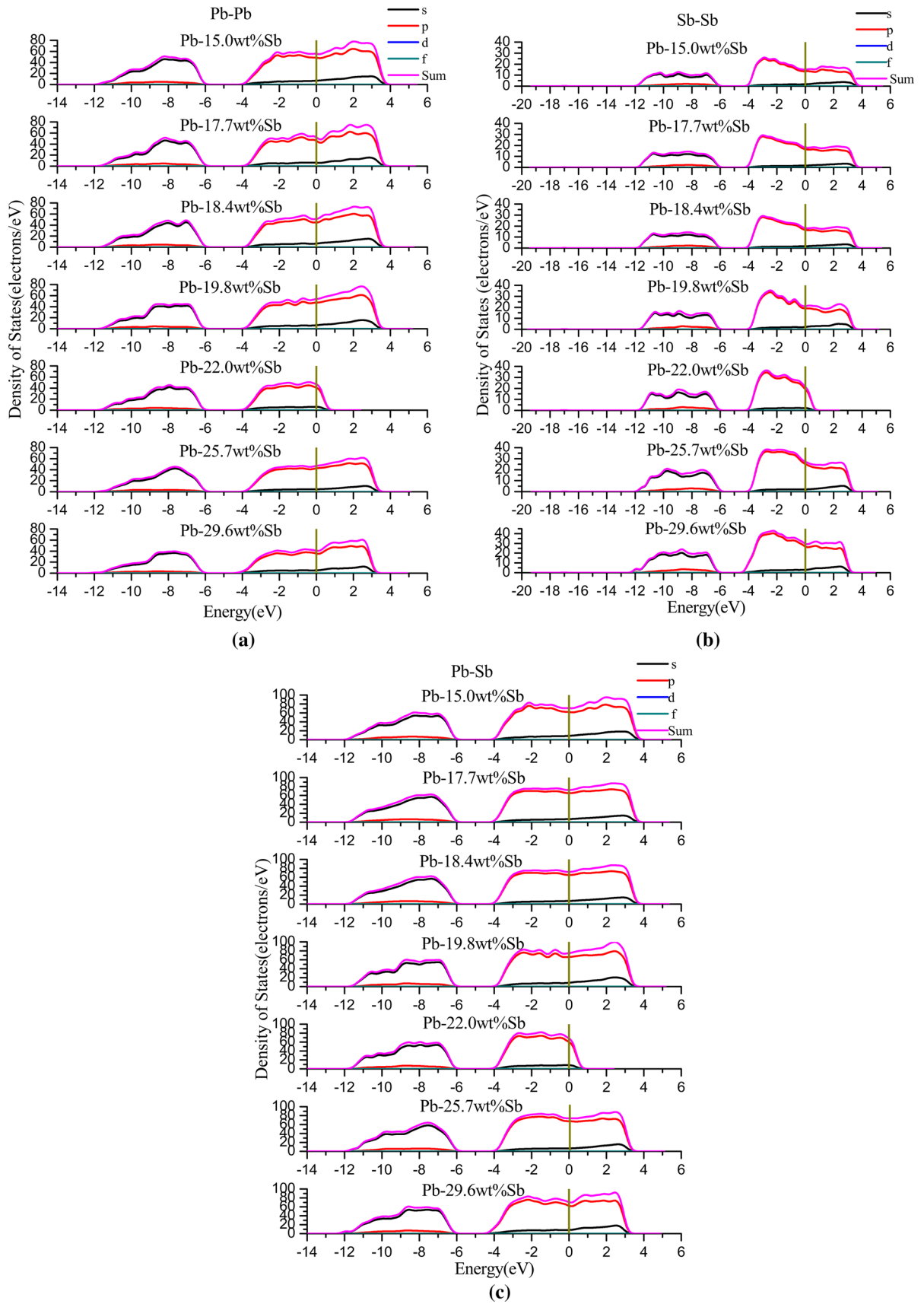


Fig. 3—Partial density of states of 7 kinds of Pb-Sb alloys at 1073 K (800 °C): (a) Pb-Pb; (b) Sb-Sb; (c) Pb-Sb.

**Table II. The Quantitative Analysis Results of Pb-Sb Alloy After Vacuum Distillation at 1073 K (800 °C)**

Compositions	Experimental Number	Distillation Time (min)	Residue (Pct)		Volatile (Pct)		The Ratio of Pb/Sb in Residue	The Ratio of Pb/Sb in Volatile
			Pb	Sb	Pb	Sb		
Pb-11.2 pctSb	1	90	77.80	20.90	89.20	10.10	3.72	8.83
	2	120	74.50	24.10	89.30	11.50	3.09	7.77
	3	150	84.60	13.41	86.13	9.59	6.31	8.98
Pb-16.5 pctSb	4	90	81.32	18.89	78.45	18.75	4.30	4.18
	5	120	82.98	16.02	73.29	17.05	5.18	4.30
	6	150	83.04	16.51	80.35	17.63	5.03	4.56
Pb-20 pctSb	7	90	83.62	15.46	72.70	24.45	5.41	2.97
	8	120	80.10	15.10	72.90	18.90	5.30	3.86
	9	150	81.10	16.90	69.90	25.70	4.80	2.72
Pb-22 pctSb	10	90	84.26	14.78	70.18	27.76	5.70	2.53
	11	120	84.80	15.76	72.77	25.54	5.38	2.85
	12	150	84.54	15.84	75.05	23.92	5.34	3.14
Pb-50 pctSb	13	90	68.70	30.70	32.80	66.40	2.24	0.49
	14	120	70.30	22.20	51.90	48.40	3.17	1.07
	15	150	79.72	15.40	39.55	59.34	5.18	0.67

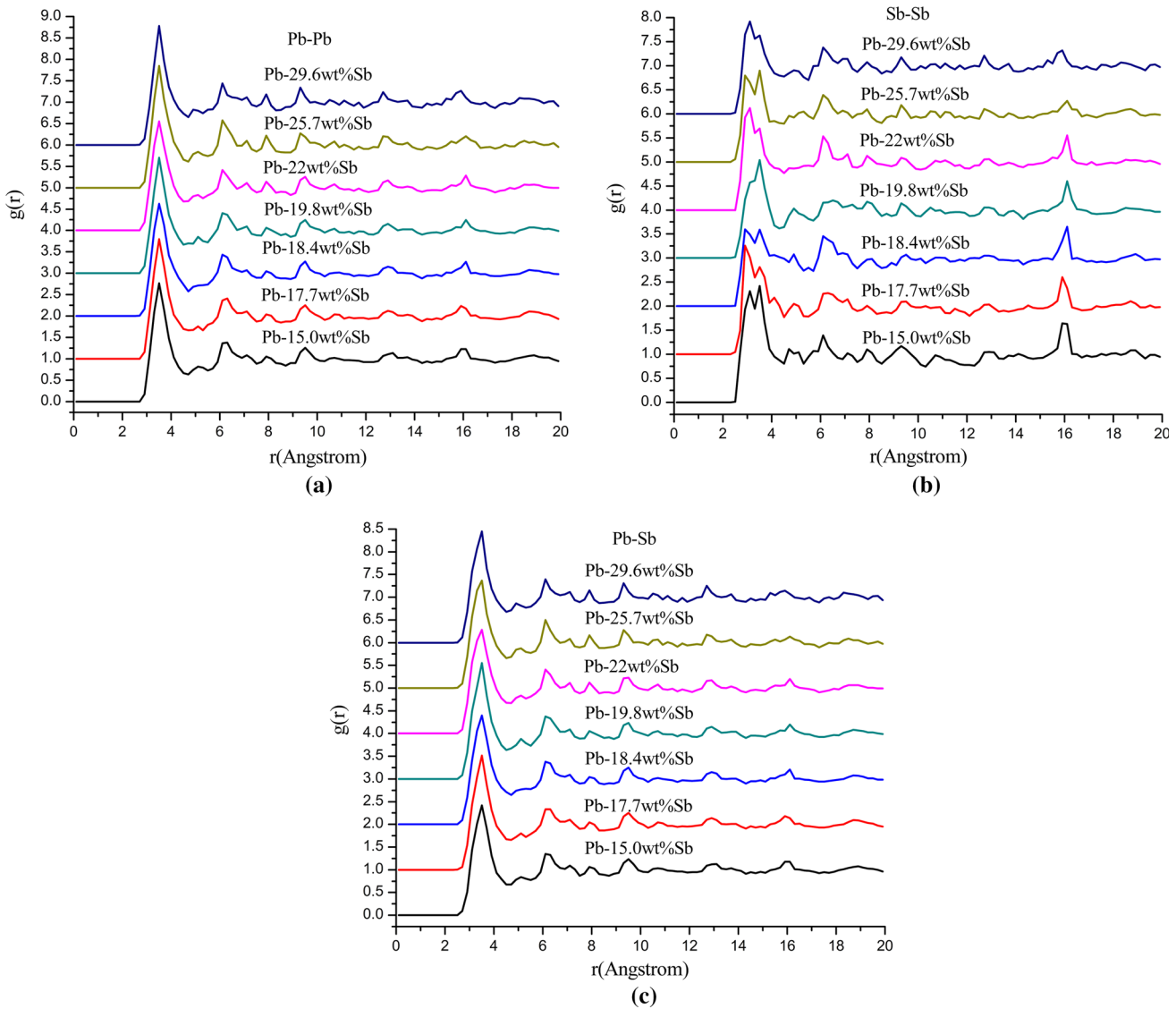


Fig. 4—Calculated pair correlation functions  $g(r)$  of liquid Pb-Sb alloys at 1073 K (800 °C): (a) Pb-Pb; (b) Sb-Sb; (c) Pb-Sb.

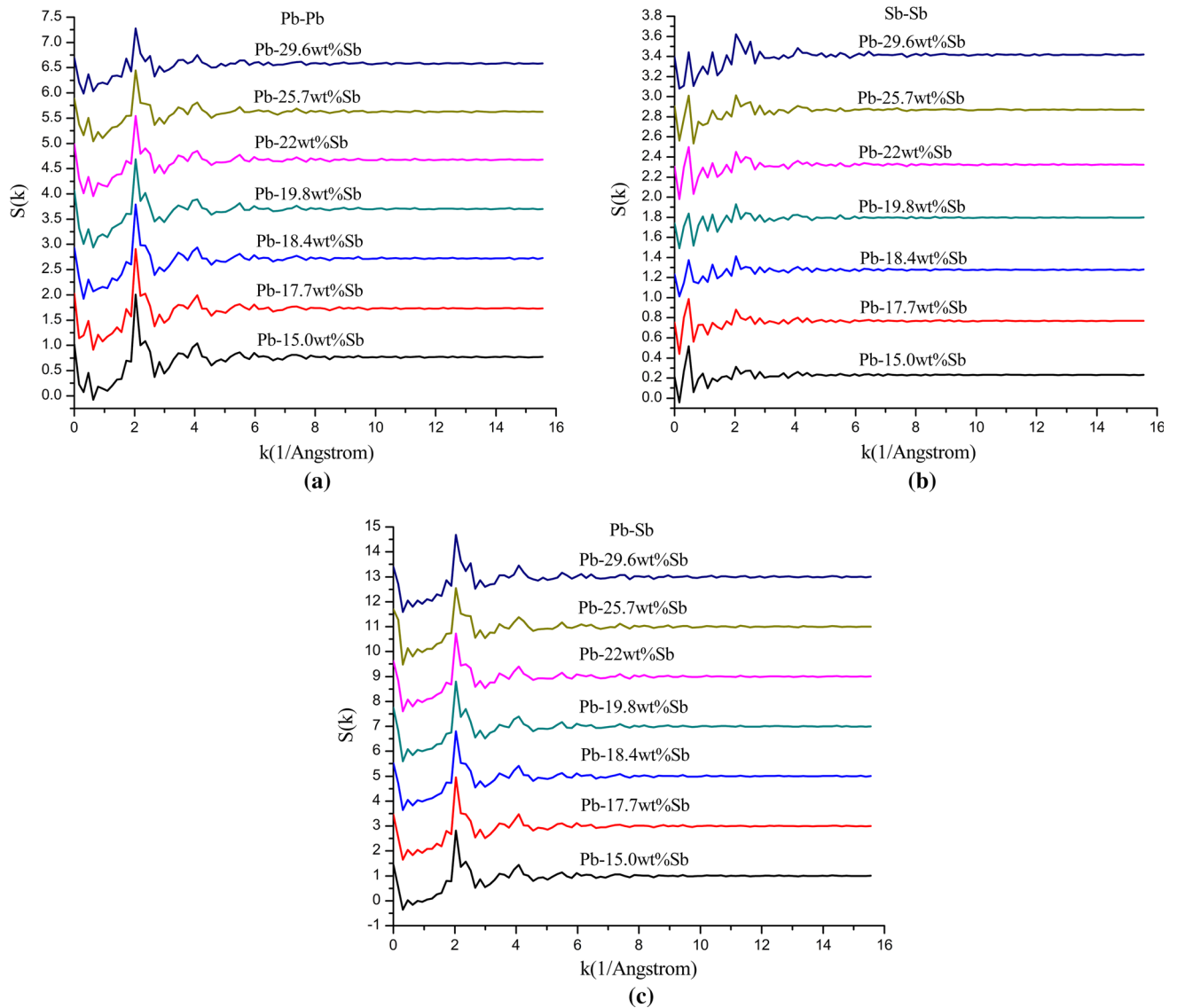


Fig. 5—Calculated partial structure factor  $S(k)$  of liquid Pb-Sb alloys at 1073 K (800 °C): (a) Pb-Pb; (b) Sb-Sb; (c) Pb-Sb.

to the narrow band, which indicates the localization of electrons, then the interaction between atoms strengthens, so it is difficult to separate with experiment.

## 2. Structural properties

*a. Partial radial distribution function.* Partial PDFs of Pb-Pb, Sb-Sb, and Pb-Sb pairs for different compositions are shown in Figure 4, respectively. PDFs of pure Pb and Sb are also exhibited for comparison.

As seen from Figure 4, there are three peaks located at about 3.50, 4.90 to 5.10, and 6.10 Å, respectively. Two troughs between these three peaks are relatively shallow. The first peaks in  $g_{\text{Pb-Pb}}(r)$  and  $g_{\text{Pb-Sb}}(r)$  are symmetrical, and their positions are almost independent of concentration. While the first peak in  $g_{\text{Sb-Sb}}(r)$  is asymmetrical, and the main peak is split into two well-defined peaks indicating a more complex structure,<sup>[29]</sup> and the position of the main peak shifts from

$r = 3.5 \text{ \AA}$  at 19.8 wt pct Sb to  $r = 3.1 \text{ \AA}$  at 22 wt pct Sb. Its pair correlation function is more complex with a small shoulder on the right-hand side of the main peak, which indicates that there are covalent bonds surviving in Sb-Sb.<sup>[24]</sup> Agreement with the *ab initio* simulation result of *l*-Sb by Seifert<sup>[30]</sup> is good.

The first trough (between the first peak and the second one) becomes shallower firstly, and the height of second peak decreases with the increase of Sb content, which makes the second peak change into a shoulder in 18.4 wt pctSb (22 wt pctSb) for  $g_{\text{Pb-Pb}}(r)$ ,  $g_{\text{Pb-Sb}}(r)$  ( $g_{\text{Sb-Sb}}(r)$ ), respectively. The second peak reappears abnormally in 19.8 wt pctSb (25.7 wt pctSb), and then it decreases again with the increase of Sb content, indicating that an abnormal structural change may occur in the temperature range from 18.4 wt pctSb (22 wt pctSb) to 19.8 wt pctSb (25.7 wt pctSb). In addition, in Pb-22 wt pctSb, the first peak is high and trough of the first trough would almost be shoulder, showing

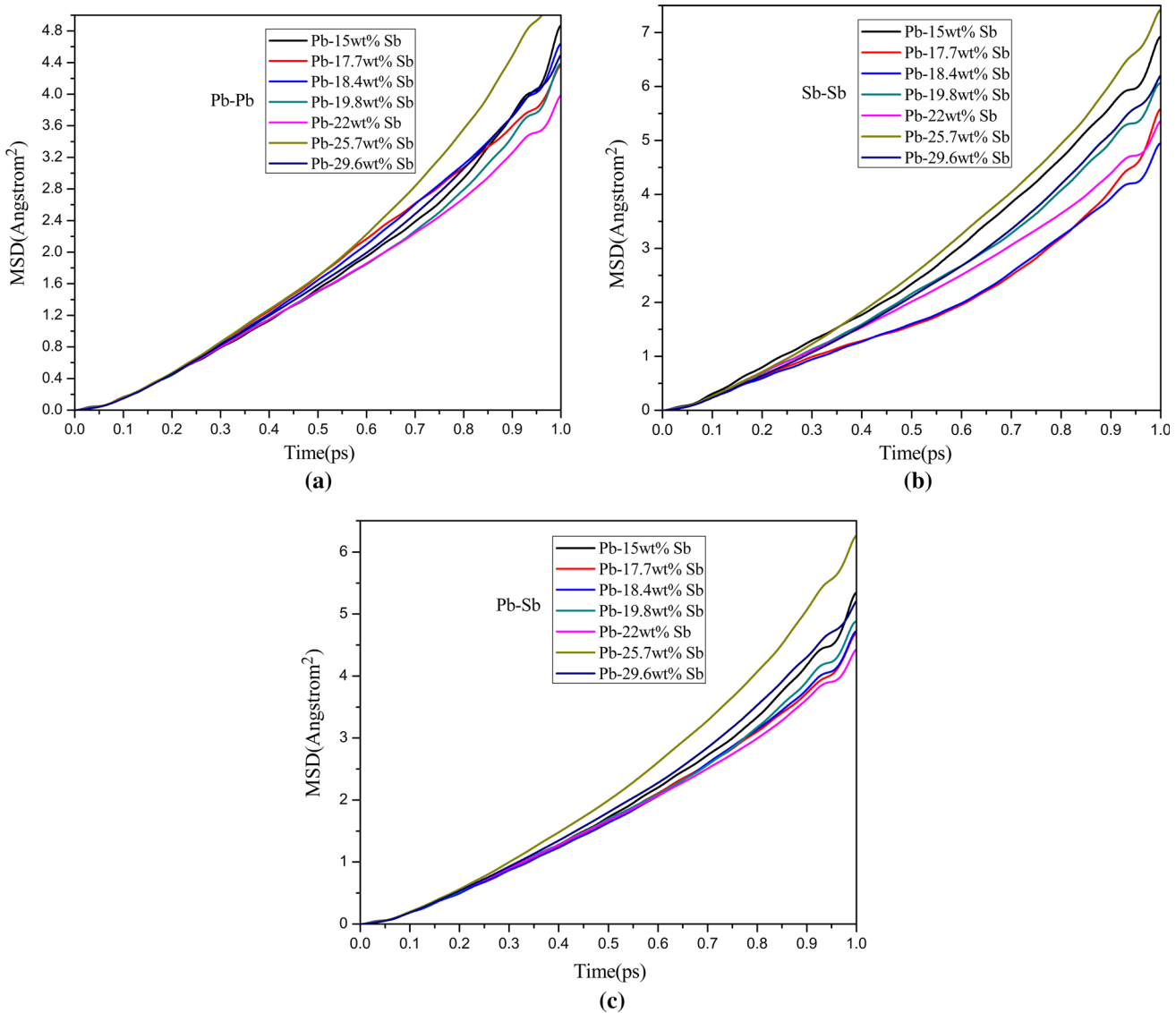


Fig. 6—The variation of MSD versus time for Pb-Sb alloys at 1073K (800°C): (a) Pb-Pb; (b) Sb-Sb; (c) Pb-Sb.

that the degree of order is higher than several other components.<sup>[28]</sup>

*b. Structure factor.* To discuss the short- or medium-range ordering of Pb and Sb atoms, it is useful to investigate the concentration-concentration structure factor  $S(k)$ . Figure 5 shows the calculated structure factors of Pb-Sb alloys.

In this figure, the structure factor displays a main peak at  $k = 2.04 \text{ \AA}^{-1}$ , a shoulder can be found around  $2.3 \text{ \AA}^{-1}$  on the right side of the first peak in  $S(k)$ , which implies a nonsimple local structure in the liquid is a symbol of local ordering resulting from covalent bonding of the anisotropy in the liquid.<sup>[24,31]</sup>

There is a pronounced first peak (so called prepeak) at about  $0.47 \text{ \AA}^{-1}$ , in accordance with the literature,<sup>[32,33]</sup> indicating the presence of heterogeneous clusters in the liquid and the medium-range ordering in the melt.<sup>[18,34]</sup> Besides, the position of the prepeak of  $S(k)$  at  $k \approx 0.47 \text{ \AA}^{-1}$  conforms to the distance  $r \approx 6.1 \text{ \AA}$  using

the rule of thumb  $k_r = 7.7$ . This distance coincides with the position of the second peak of  $g_{\text{Pb-Pb}}(r)$ , which means that of Pb atoms gives rise to the prepeak of the  $S_{\text{Pb-Pb}}(k)$ .<sup>[35]</sup> Meanwhile, the height of prepeak increases with the increase of Sb content and the maximum value appearing at 22 wt pctSb, indicating that degree of disorder reduces and degree of order is supreme in the system.

*c. Mean square displacement.* We studied the atomic diffusion in the liquid by calculating the time-dependent mean square displacement (MSD) defined for species  $\alpha$  as<sup>[36,37]</sup>

$$\langle \Delta r_\alpha(t)^2 \rangle = \frac{1}{N_\alpha} \left\langle \sum_{i=1}^{N_\alpha} |r_{\alpha i}(t + t_0) - r_{\alpha i}(t_0)|^2 \right\rangle, \quad [2]$$

where the sum goes over all  $N_\alpha$  atoms of species  $\alpha$ ,  $t_0$  is an arbitrary time origin, and the angular brackets  $\langle \rangle$  denote a thermal average or equivalently an average

**Table III. The Diffusion Coefficients of Lead-Antimony Alloy with Different Components at 1073 K (800 °C)**

Composition	$D_{\text{Pb}}$ ( $10^{-8} \text{ m}^2 \text{ s}^{-1}$ )	$D_{\text{Sb}}$ ( $10^{-8} \text{ m}^2 \text{ s}^{-1}$ )	$D_{\text{Sb-Pb}}$ ( $10^{-8} \text{ m}^2 \text{ s}^{-1}$ )	$D_{\text{Sb}}/D_{\text{Pb}}$
Pb-15.0 wt pctSb	0.7310	1.0973	0.8158	1.5011
Pb-17.7 wt pctSb	0.7724	0.7803	0.7345	1.0102
Pb-18.4 wt pctSb	0.7426	0.7526	0.7454	1.0135
Pb-19.8 wt pctSb	0.6751	0.9647	0.7609	1.4290
Pb-22 wt pctSb	0.6345	0.8473	0.7035	1.3354
Pb-25.7 wt pctSb	0.8838	1.1994	1.0001	1.3571
Pb-29.6 wt pctSb	0.7314	1.0045	0.8452	1.3734

over time origins. The calculated results are shown in Figure 6. For diffusing liquids, the MSD is linear in time, and the slope is proportional to the diffusion coefficient  $D_\alpha$ ,  $\langle \Delta r_\alpha(t)^2 \rangle \rightarrow 6D_\alpha t + A_\alpha$ , where  $A_\alpha$  is the constant.

The diffusion coefficient ( $D_{\text{Pb}}$ ,  $D_{\text{Sb}}$ , and  $D_{\text{Sb-Pb}}$ ) and the  $D_{\text{Sb}}/D_{\text{Pb}}$  are listed in Table III. In all calculation results, the  $D_{\text{Sb}}$  is larger than  $D_{\text{Pb}}$ . In general, self-diffusion coefficients are sensitive to the change of liquid structure and can be served as another way to study the microstructure of liquid.<sup>[38]</sup>  $D_{\text{Pb}}$ ,  $D_{\text{Sb}}$  and  $D_{\text{Sb-Pb}}$  firstly decreases and then increases with the increasing Sb content, there is a minimum value in Pb-22 wt pctSb. This minimum value implies strong binding between Pb and Sb, which this ingredient cannot be separated. In addition, because the mass of Sb atom is smaller than that of Pb atom, the smaller ratio of  $D_{\text{Sb}}/D_{\text{Pb}}$  indicates that the Pb and Sb atoms have stronger correlations between them.<sup>[37]</sup>

## V. CONCLUSIONS

We have carried out AIMDs for the liquid Pb-Sb alloys to investigate the composition dependence of their ionic structure and electronic states, and obtained the following results:

Our investigations of the electronic structures show that there is no gap at the Fermi level in PDOS of Pb-Sb, Pb-Pb, and Sb-Sb, demonstrating metallic behavior. In Pb-22 wt pctSb, the composition point with the lowest energy is most stabilized. We have also calculated the diffusion coefficients for Pb and Sb atoms, which show that the interaction between Pb and Sb atoms is strong in Pb-22 wt pctSb since the diffusion coefficient value is minimum. And on the basis of the experiments, it has been proved that there exists common volatilization for Pb-Sb alloys when Sb content is 16.5 wt pctSb. The experimental and calculations results suggest that there is common volatilization phenomenon in Pb-Sb alloys, and the azeotropic point is Pb-22 wt pctSb.

## ACKNOWLEDGMENTS

The authors are grateful for the financial support from the Cultivating Plan Program for the Technological Leading Talents of Yunnan Province (2014HA003), the National Natural Science Founda-

tion of China and Project (Grant No. 51474116, 51104079, 51104078), the Joint Program of Natural Science Foundation of China and Yunnan Province (Grant U1202271), the Program for Innovative Research Team in University of Ministry of Education of China (Grant No. IRT1250), the Program for Innovative Research Team in Nonferrous Metal Vacuum Metallurgy of Ministry of Science and Technology (Grant No. 2014RA4018), and the Fundamental Research of Yunnan province (Grant No. 2013FZ033).

## REFERENCES

1. L.X. Kong, B. Yang, B.Q. Xu, and Y.F. Li: *Metall. Mater. Trans. A*, 2014, vol. 45A, pp. 4405–10.
2. Y.N. Dai and B. Yang: *Vacuum metallurgy for nonferrous metals and materials*, Metallurgical Industry Press, Beijing, 2009 [in Chinese].
3. F. Chen, Z.K. He, and Y.N. Dai: *J. Kunming Inst. Technol.*, 1984, vol. 3, pp. 108–16 [in Chinese].
4. G.J. Zhang, Y.C. Liu, and Y.N. Dai: *Nonferrous Met. (Extr. Metall.)*, 1989, vol. 4, pp. 21–22 [in Chinese].
5. G.J. Zhang, Y.C. Liu, and Y.N. Dai: *J. Kunming Inst. Technol.*, 1989, vol. 14, pp. 68–76 [in Chinese].
6. Y.N. Dai and G.J. Zhang: *Trans. Nonferrous Met. Soc. China*, 1991, vol. 1, pp. 39–44 [in Chinese].
7. B. Yang, Y.N. Dai, and G.J. Zhang: *Yunnan Metall.*, 1999, vol. 28, pp. 40–43 [in Chinese].
8. X. J. Zhang: *Kunming University of Science and Technology*, Kunming, 1983 [in Chinese].
9. J. Hu: *Kunming University of Science and Technology Kunming*, 1996 [in Chinese].
10. W.J. Kroll: *Trans. Electrochem. Soc.*, 1945, vol. 87, pp. 571–87.
11. R. Kumar and C.S. Sivaramakrishnan: *J. Mater. Sci.*, 1969, vol. 4, pp. 383–88.
12. F.X. Guo, W. Wang, H.L. Yang, J.Y. Qin, and X.L. Tian: *Trans. Nonferrous Met. Soc. China*, 2012, vol. 22, pp. 3113–19.
13. X.F. Bian, H. Li, L. Zhang, and J.J. Ma: *Chin. Sci. Bull.*, 1996, vol. 41, pp. 873–78.
14. Z.T. Fidkowski, M.F. Malone, and M.F. Doherty: *Comput. Chem. Eng.*, 1993, vol. 17, pp. 1141–55.
15. Y. Senda, F. Shimojo, and K. Hoshino: *J. Phys. Soc. Jpn.*, 1998, vol. 67, pp. 916–21.
16. G.A. De Wijs, G. Pastore, A. Selloni, and W. Van der Lugt: *J. Chem. Phys.*, 1995, vol. 103, pp. 5031–40.
17. G. Seifert, R. Kaschner, M. Schöne, and G. Pastore: *J. Phys. Condens. Matter*, 1998, vol. 10, pp. 1175–98.
18. C.Q. Zhang, Y.H. Wei, and C.F. Zhu: *Chem. Phys. Lett.*, 2005, vol. 408, pp. 348–53.
19. Q.H. Hao, W. Liu, Y.D. Li, and C.S. Liu: *J. Non-Cryst. Solids*, 2010, vol. 356, pp. 8–13.
20. J.M. Holender and M.J. Gillan: *Phys. Rev. B*, 1995, vol. 53, pp. 4399–407.
21. K. Seifert-Lorenz and J. Hafner: *Phys. Rev. B*, 1999, vol. 59, pp. 843–54.
22. Y. Senda, F. Shimojo, and K. Hoshino: *J. non-cryst. solids*, 1999, vol. 250, pp. 258–62.



23. D.P. Tao: *Thermochim. Acta*, 2000, vol. 363, pp. 105–13.
24. T.K. Gu, X.F. Bian, J.Y. Qin, and C.Y. Xu: *Phys. Rev. B*, 2005, vol. 71, pp. 104206-1–104206-8.
25. W. Jank and J. Hafner: *Phys. Rev. B*, 1990, vol. 41, pp. 1497–515.
26. F. Knider, J. Hugel, and A.V. Postnikov: *J. Phys. Condens. Matter*, 2007, vol. 19, pp. 196105-1–196105-12.
27. MMG Alemany, RC Longo, LJ Gallego, DJ González, LE González, L Tiago Murilo, and R Chelikowsky James: *Phys. Rev. B*, 2007, vol. 76, pp. 214203-1–214203-7.
28. Q.H. Hao, Y.D. Li, X.S. Kong, and C.S. Liu: *Int. J. Mod. Phys. B*, 2013, vol. 27, pp. 1350012-1–1350012-10.
29. C. Bergman, M.V. Coulet, R. Bellissent, K. Seifert-Lorenz, and J. Hafner: *J. Non-cryst. Solids*, 1999, vol. 250, pp. 253–57.
30. K. Seifert, J. Hafner, and G. Kresse: *J. Non-cryst. Solids*, 1996, vols. 205–207, pp. 871–74.
31. T. Itami, S. Munejiri, T. Masaki, H. Aoki, Y. Ishii, T. Kamiyama, Y. Senda, F. Shimojo, and K. Hoshino: *Phys. Rev. B*, 2003, vol. 67, pp. 064201-1–064201-12.
32. J.Y. Qin, X.F. Bian, W.M. Wang, J.J. Ma, and C.Y. Xu: *Chin. Sci. Bull.*, 1998, vol. 43, pp. 1445–50.
33. H.R. Wang, Y.F. Ye, and G.H. Min: *Metallofiz. i noveishie tekhnologii*, 2001, vol. 23, pp. 727–34.
34. H. Neumann and A. Mikula: *J. Non-Cryst. Solids*, 2002, vols. 312–314, pp. 30–33.
35. W. Van der Lugt: *J. Phys. Cond. Matter*, 1996, vol. 8, pp. 6115–38.
36. P.A. Egelstaff: *An introduction to the liquid state*, Clarendon, New York, 1992, p. 240.
37. T.K. Gu, J.Y. Qin, X.F. Bian, C.Y. Xu, and Y.H. Qi: *Phys. Rev. B*, 2004, vol. 70, pp. 245214-1–7.
38. G.X. Qian, M. Weinert, G.W. Fernando, and J.W. Davenport: *Phys. Rev. Lett.*, 1990, vol. 64, pp. 1146–49.